

Synthesis, structure and characterization of novel nickel(II) and iron(II) complexes with a 5,5'-bis[2-(2,2'-bipyridin-6-yl)-ethyl]-2,2'-bipyridine ligand

Mou-Hai Shu, Chun-Ying Duan, Wei-Yin Sun,* You-Jun Fu, Dao-Hua Zhang, Zhi-Ping Bai and Wen-Xia Tang*

State Key Laboratory of Coordination Chemistry, Coordination Chemistry Institute, Nanjing University, Nanjing 210093, China

Received 9th March 1999, Accepted 28th May 1999

A new tris-bipyridine ligand 5,5'-bis[2-(2,2'-bipyridin-6-yl)-ethyl]-2,2'-bipyridine (L) was synthesized, and complexes $[ML_3][PF_6]_2 \cdot 2EtOH \cdot 0.5H_2O$ [$M = Ni(II)$, **1**; $M = Fe(II)$, **2**] were obtained by reaction of the ligand L with Ni(II) and Fe(II) ions, respectively. X-Ray data of complex **1** show that the central 5,5'-disubstituted 2,2'-bipyridine units of each ligand L coordinate to the Ni(II) ion to give a distorted octahedral environment, while all the terminal 6-monosubstituted 2,2'-bipyridine groups of the ligand keep free of coordination. Complex **2** is isomorphic to **1**. The solution behavior of complex **2** was investigated by 1H NMR spectroscopy. Complexes **1** and **2** were also characterized by ES-MS spectrometry and cyclic voltammetry. The ES-MS spectral data indicate that only the mononuclear complexes formed in the reaction mixtures of the ligand L and $M(ClO_4)_2$ ($M = Fe$ and Ni) even in the presence of excess metal ion. The results illustrate that the central 5,5'-disubstituted 2,2'-bipyridine moiety of each ligand L is selectively coordinated by octahedral geometric metal ions, whereas the 6-substituted 2,2'-bipyridine unit does not participate in any metal ion coordination.

Introduction

Oligobipyridine ligands with different spacer groups and different linkage modes have been widely used in the study of the assembly of supramolecules in recent years.¹⁻⁴ For example, 1,2-bis(2,2'-bipyridin-6-yl)ethane coordinates to Cu(II) in a tetradentate mode to give a mononuclear complex.³ In the case of a tris-2,2'-bipyridine ligand with 4,4'- and 6,6'-disubstituted 2,2'-bipyridine units, the terminal 4,4'-disubstituted 2,2'-bipyridine moieties are selectively coordinated by $Ru(bipy)_2$ ($bipy = 2,2'$ -bipyridine), whereas the central 6,6'-disubstituted 2,2'-bipyridine units do not participate in any metal ion coordination.⁴ However, oligobipyridine ligands containing 6,6'- or 5,5'-disubstituted 2,2'-bipyridine result in the formation of double- and triple-stranded helices⁵⁻¹⁰ or novel circular double helical complexes.^{11,12} Therefore it appears that the linkage mode of the spacer group to the bipyridine units in the oligobipyridine ligands plays an important role in the binding behavior of the 2,2'-bipyridine group. In order to further illustrate this argument, we designed and synthesized a new ligand L, in which three bipyridine units are bridged by a CH_2CH_2 group at the 5 and 6'-positions, *i.e.* the central bipyridine unit is 5,5'-disubstituted and terminal bipyridine units are 6-mono-substituted as shown schematically below (Scheme 1), and the

reactions between L and Ni(II) and Fe(II) were investigated. The results show that the oligobipyridine ligand L coordinates to Ni(II) and Fe(II) with the central 5,5'-disubstituted 2,2'-bipyridine moiety to form mononuclear complexes and the terminal 6-monosubstituted 2,2'-bipyridine units are pendant. The results indicate that the linkage mode of the spacer group to the bipyridine units in the oligobipyridine ligands influence the assembly of the supramolecules as well as the binding of the 2,2'-bipyridine group.

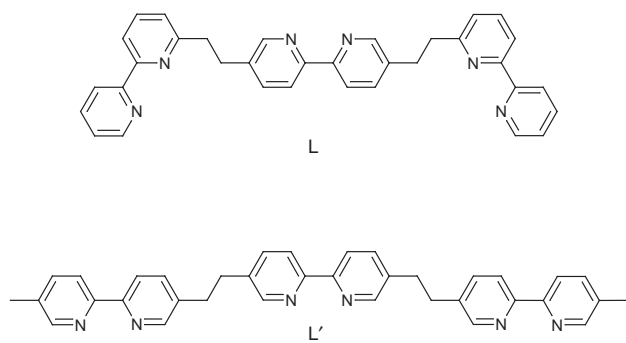
Experimental

Materials

Anhydrous THF was refluxed with sodium-benzophenone and distilled before use. 6-Methyl-2,2'-bipyridine³ and 5,5'-bis(bromomethyl)-2,2'-bipyridine¹³ were synthesized according to the literature methods. Acetonitrile was purified by treatment with $KMnO_4$ and then distilled over P_2O_5 and K_2CO_3 . All other chemicals were of reagent grade quality obtained from commercial sources and used without further purification.

Preparation of 5,5'-bis[2-(2,2'-bipyridin-6-yl)ethyl]-2,2'-bipyridine (L)

The ligand L was prepared by the reaction of 6-lithiomethyl-2,2'-bipyridine with 0.5 equivalents of 5,5'-bis(bromomethyl)-2,2'-bipyridine in anhydrous THF at $-78^\circ C$ under an argon atmosphere.⁸ The crude product was washed with methanol, recrystallized from $MeOH-CHCl_3$ (1/1, v/v), and purified by chromatography on silica with light petroleum (bp range: 60–90 $^\circ C$)–acetone (5:1, v/v) as eluting agent, after recrystallizing from acetonitrile, the ligand L was obtained as a pure white powder in 40% yield, mp 168–170 $^\circ C$, ES-MS: m/z , 521.3 ($M + H$)⁺, 261.5 ($M + 2H$)²⁺; 1H NMR (CD_3CN , 298 K): δ 3.23 (s, 8 H); 7.22 (d, 2 H); 7.36 (td, 2 H); 7.70 (dd, 2 H); 7.77 (t, 2H); 7.85 (td, 2H); 8.22 (d, 2 H); 8.24 (d, 2 H), 8.43 (d, 2H); 8.47 (s, 2 H), 8.65 (d, 2 H). Found: C 78.49; H 5.52; N 15.78. Calc. for $C_{34}H_{28}N_6$: C 78.43, H 5.42, N 16.15%.



Scheme 1

Preparation of [NiL₃][PF₆]₂·2EtOH·0.5H₂O **1**

60 mg of L (0.115 mmol) was suspended in ethanol (30 ml) and a solution containing 28.8 mg of Ni(OAc)₂·4H₂O (0.115 mmol) in water (4 ml) was added dropwise. The reaction mixture was refluxed with stirring for 4 hours, [NiL₃][PF₆]₂ was precipitated by addition of excess of KPF₆. The product was isolated by filtration, washed with water and diethyl ether, dried in vacuum, yield 64 mg (83%). Pink single crystals were obtained by slow evaporation from a solution of acetonitrile and methanol. Found: C 63.85; H 4.72; N 12.83. Calc. for C₁₀₆H₉₇F₁₂N₁₈NiO_{2.5}P₂: C 63.29; H 4.86; N 12.53% (the deviation may be caused by loss of the ethanol solvent molecule).

Preparation of [FeL₃][PF₆]₂·2EtOH·0.5H₂O **2**

The complex was synthesized by reaction of FeSO₄·7H₂O (0.115 mmol) with the ligand L (0.115 mmol) following the same procedures as used for the synthesis of complex **1**. The product was isolated as a dark red powder, washed with water and diethyl ether, dried in vacuum, yield 65 mg (85%). Red single crystals were obtained by slow evaporation from a solution of acetonitrile and toluene. ¹H NMR (CD₃CN, 298 K): δ 2.73 (m, 2 H), 2.85 (m, 2 H); 6.25 (s, 2 H); 6.59 (d, 2 H); 7.37 (d, 2 H); 7.45 (t, 2 H); 7.47 (t, 2 H); 7.56 (d, 2 H); 7.85 (td, 2 H); 8.13 (d, 2 H), 8.19 (d, 2 H); 8.80 (s, 2 H). Found: C 63.76; H 4.81; N 12.90. Calc. for C₁₀₆H₉₇F₁₂N₁₈FeO_{2.5}P₂: C 63.38; H 4.87; N 12.55%.

Crystallography

The diffraction intensities of complexes **1** and **2** were collected on a Siemens P4 four-circle diffractometer with graphite-monochromated Mo-K α radiation (λ =0.71073 Å) at 293(2) K using the $\omega/2\theta$ scan mode. Data were corrected for Lorentz-polarization effects during data reduction using XSCANS,¹⁴ and semi-empirical absorption correction from psi-scans was applied.

The structure of complex **1** was solved by direct methods and refined on F^2 by full-matrix least square methods using SHELXTL version 5.0.¹⁵ The PF₆⁻ anions are disordered, P–F distances were fixed at 1.540(10) Å, the site occupancy factors (s.o.f.) of these disordered fluorine atoms were refined by setting the free variable as 0.53 for F(1), F(2), F(3), F(4), F(5), F(6), and 0.47 for F(1'), F(2'), F(3'), F(4'), F(5'), F(6'), respectively. The hydrogen atoms of the water molecule were found from the difference Fourier map and refined using a riding model. The oxygen atom of the water molecule at the special position (0, 0.5, 1.0) was also refined disordered with s.o.f. = 0.25. The ethanol molecules are also disordered, the C–C distances were fixed at 1.500(20) and the C–O distances were fixed at 1.500(20) Å, the site occupancy factors were refined by setting the free variable as 0.64 for C(52), C(53), O(1), and 0.36 for C(52'), C(53'), O(1'), respectively. The other hydrogen atoms were placed in calculated positions (C–H, 0.96) assigned fixed isotropic thermal parameters at 1.2 times the equivalent isotropic U of the atoms to which they are attached and allowed to ride on their respective parent atoms. The contributions of these hydrogen atoms were included in the structure-factor calculations. All computations were carried out on a PC-586 computer using the SHELXTL-PC program package.¹⁵

Parameters for data collection and refinement of **1** are summarized in Table 1 and selected bond lengths and bond angles are listed in Table 2. Details of the structure of complex **2** are not reported because the diffraction intensities are weak and attempts to refine the structure were unsuccessful, however, the same space group and the similar cell parameters [a = 22.473(3), b = 16.880(2), c = 25.901(3) Å, β = 95.899(10)°, and V = 9773(2) Å³ at 293(2) K] indicate that complex **2** is an isomorph of complex **1**.

CCDC reference number 186/1477.

Table 1 Summary of crystal data, data collection and structure refinement for complex **1**

Empirical formula	C ₁₀₆ H ₉₇ F ₁₂ N ₁₈ NiO _{2.5} P ₂
Formula weight	2011.67
T/K	293(2)
Crystal system	Monoclinic
Space group	$C2/c$
$a/\text{Å}$	22.705(8)
$b/\text{Å}$	16.885(2)
$c/\text{Å}$	25.917(4)
$\beta/^\circ$	96.44(2)
$U/\text{Å}^3$, Z	9856(4), 4
μ/mm^{-1}	0.313
Measured/Independent reflections	9717/8272, [R_{int} = 0.0519]
R_1	0.0720
wR_2 , wR_2 (for all data)	0.1735, 0.2258

Table 2 Selected bond lengths (Å) and angles (°) for complex **1**

Ni(1)–N(3)	2.104(3)	Ni(1)–N(3) ^a	2.104(3)
Ni(1)–N(4)	2.083(3)	Ni(1)–N(4) ^a	2.083(3)
Ni(1)–N(9)	2.100(3)	Ni(1)–N(9) ^a	2.100(3)
N(3)–Ni(1)–N(4)	78.88(14)	N(4)–Ni(1)–N(9) ^a	90.76(12)
N(3)–Ni(1)–N(9)	172.30(13)	N(9)–Ni(1)–N(3) ^a	95.29(13)
N(3)–Ni(1)–N(3) ^a	91.3(2)	N(9)–Ni(1)–N(4) ^a	90.76(12)
N(3)–Ni(1)–N(4) ^a	94.43(13)	N(9)–Ni(1)–N(9) ^a	78.4(2)
N(3)–Ni(1)–N(9) ^a	95.29(13)	N(3) ^a –Ni(1)–N(4)	78.88(14)
N(4)–Ni(1)–N(9)	96.60(13)	N(3) ^a –Ni(1)–N(9)	172.29(13)
N(4)–Ni(1)–N(3) ^a	94.43(13)	N(4) ^a –Ni(1)–N(9)	96.60(13)
N(4)–Ni(1)–N(4) ^a	170.5(2)		

Symmetry transformations used to generate equivalent atoms: ^a $-x, y, -z + 3/2$.

See <http://www.rsc.org/suppdata/dt/1999/2317/> for crystallographic files in .cif format.

ES-MS spectral measurement

Complexes **1** and **2** were dissolved in 1:1 (v/v) acetonitrile–water, with the approximate concentration 0.01 mmol L⁻¹. The other samples were prepared by the following procedures: 1.00 ml of ligand L in acetonitrile (1.0 mg ml⁻¹) was mixed with a measured portion of freshly prepared standardised M(ClO₄)₂ solutions (M = Fe and Ni) in water, and the resulting mixtures were stirred for 4 hours at 70 °C to give clear solutions. Electro-spray mass spectra (ES-MS) were measured on a LCQ system (Finnigan MAT, USA) using methanol as the mobile phase. The spray voltage, tube lens offset, capillary voltage and capillary temperature were set at 4.50 kV, 0 V, 17.00 V and 150 °C, respectively. The quoted m/z values represent the major peaks in the isotopic distribution.

Molecular modeling

Cerius² (Version 3.5)¹⁶ software program from Molecular Simulation Inc. was employed to do the molecular modeling. Dynamic calculations and energy minimization were carried out using the Universal forcefield¹⁷ which is an open forcefield (OFF).

Other physical measurements

¹H NMR spectra were recorded on a Bruker AM-500 spectrometer using the residual proton in deuterated solvent as internal reference (CD₃CN, 1.93 ppm). Electrochemical measurements were performed on an EG&G M273 potentiostat/galvanostat system using a platinum disk working electrode (0.008 cm²), which was polished prior to use and rinsed thoroughly with water and acetone, a platinum wire counter electrode and an Ag–AgCl electrode used as reference. All the measurements were carried out at 298 K in argon-purged (dioxxygen-free) acetonitrile solutions with 0.1 M freshly

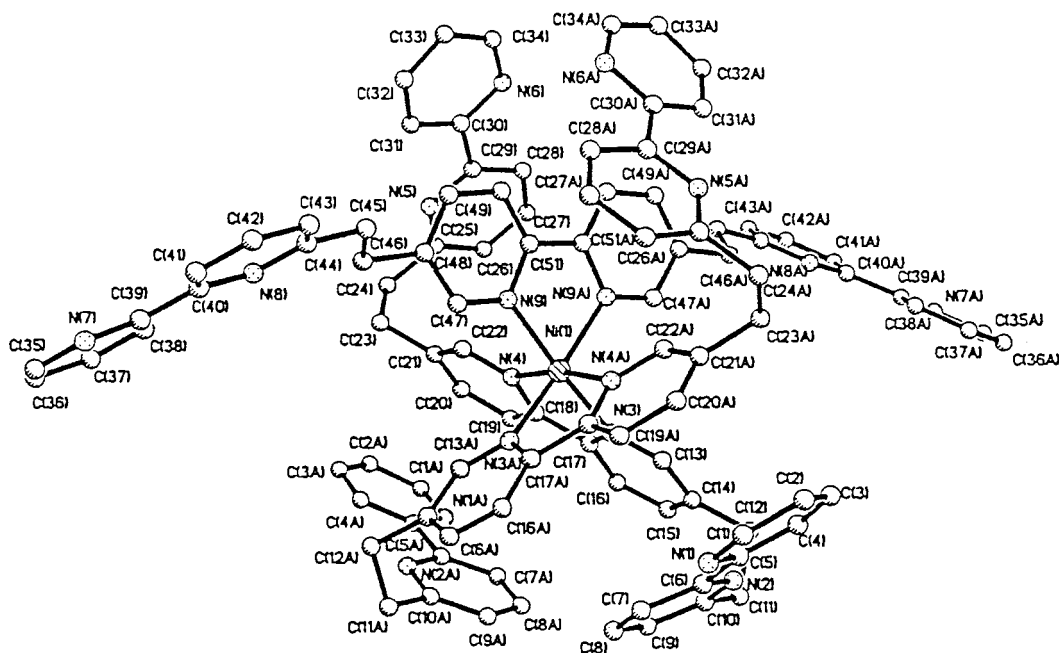


Fig. 1 The structure of the cation $[\text{NiL}_3]^{2+}$ with atom numbering scheme. All the hydrogen atoms were omitted for clarity.

recrystallized tetra-*n*-butylammonium perchlorate $[(\text{TBA})\text{ClO}_4]$ as supporting electrolyte. The scan rate was 100 mV s^{-1} . Ferrocene was added at the end of each experiment as an internal reference.

Results and discussion

The crystal structure of complex 1

Fig. 1 shows the structure of cation part $[\text{NiL}_3]^{2+}$ of complex 1 with the atom numbering scheme. The central 5,5'-disubstituted bipyridine units of each ligand coordinate the Ni(II) ion, while all the terminal 6-monosubstituted bipyridine units of the ligand keep free of coordination. The central Ni(II) ion has a distorted octahedral coordination sphere. The Ni–N distances vary from 2.083(3) to 2.104(3) Å. The *cis*-N–Ni–N bond angles vary from 78.4(2) to 96.60(13)° and from 170.5(2) to 172.29(13)° for the *trans* as listed in Table 2. The Ni(II) center is a tris-(bipyridine) complex with D_3 local symmetry ignoring the terminal substituted 2,2'-bipyridine groups of each ligand. The two-fold rotation axis passes through the Ni(II) ion and the center between N(9) and N(9A) atoms, the corresponding two-fold rotation symmetry operation can generate the other half of the molecule.

Each pyridine ring is planar with a maximum deviation of 0.03 Å, and the bipyridine fragments in each ligand L are almost planar as reflected by their dihedral angles [N(1)/N(2): 6.3; N(3)/N(4): 1.9; N(5)/N(6): 8.0; N(7)/N(8): 4.6; N(9)/N(9A): 4.7° the pyridine rings are numbered according to the nitrogen atom as shown in Fig. 1]. The dihedral angles between the bipyridine units are 59.8° for N(1),N(2)/N(3),N(4), 63.7° for N(3),N(4)/N(5),N(6), and 69.7° for N(7),N(8)/N(9),N(9A), or N(7A),N(8A)/N(9),N(9A), respectively (the bipyridine planes were named after the nitrogens they contained). The torsion angles are -68.8° for C(10)–C(11)–C(12)–C(14), and -54.7° for C(21)–C(23)–C(24)–C(25) whereas the C–CH₂–CH₂–C torsion angle in the strand containing N(9), N(9A) is -171.8° for C(44)–C(45)–C(46)–C(48). It is different from those in the other two ligand strands as just mentioned. It can be seen from Fig. 1 that the strands containing N(3),N(4), and N(3A),N(4A) are intertwined around the Ni(II) ion while the strand containing N(9),N(9A) adopts an almost linear arrangement.

In complex 1, all the terminal 6-monosubstituted bipy units of the three ligands keep free of coordination. However, in the

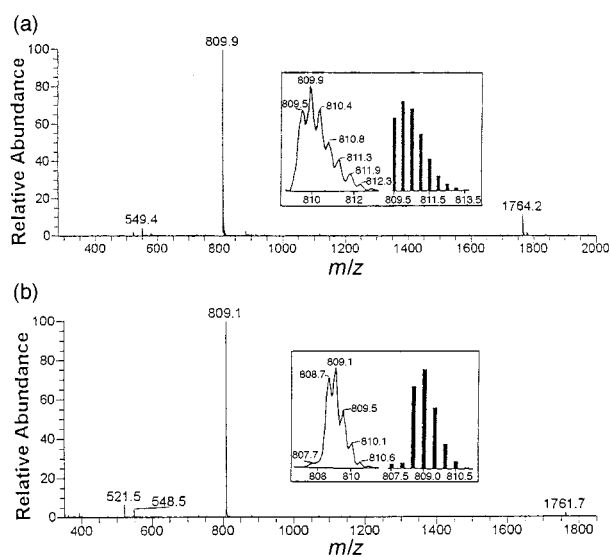


Fig. 2 (a) Electropray mass spectrum of complex 1, (b) Electropray mass spectrum of complex 2, the insets show the comparison of the observed (traces) and calculated (bars) isotopic distributions for the base peaks observed in the ES-MS spectra of the complexes.

case of the 5,5'-disubstituted tris-bipyridine ligand (L') (see Scheme 1) the triple-stranded helical complex has been obtained with the same nickel(II) ion. The absence of the trinuclear triple-stranded helicate species M_3L_3 with the ligand L is considered to be caused by the steric hindrance of the methylene substituents alpha to the chelating nitrogens of the terminal bipyridine units. Balzani and co-workers have obtained similar results⁴ in which the central 6,6'-substituted bipyridine unit does not participate in the coordination with $[\text{Ru}(\text{bpy})_2]^{2+}$ (bpy = bipyridine), PdCl_2 , ZnBr_2 and $\text{Hg}(\text{CF}_3\text{-CO}_2)_2$ and only the terminal 4,4'-disubstituted 2,2'-bipyridine moieties coordinate to the metal ions.

Electropray mass spectra of the complexes

The electropray mass spectra (ES-MS) of complexes 1 and 2 are shown in Fig. 2. The spectrum of complex 1 displays three peaks [Fig. 2(a)], a base peak at m/z 809.9 in which the isotopic distribution patterns separated by 0.5 ± 0.1 dalton correspond

to the major species present: $[\text{NiL}_3]^{2+}$, a small peak at m/z 1764.2 with 1.0–1.1 dalton separated isotopic distribution patterns results from the cation $\{[\text{NiL}_3][\text{PF}_6]\}^+$, and another small peak at m/z 549.4 corresponds to $[\text{NiL}_2]^{2+}$. As shown in Fig. 2(b), the ES-MS spectrum of **2** includes four main peaks, a peak at m/z 809.1 corresponding to the most abundant double cation $[\text{FeL}_3]^{2+}$, a peak at m/z 1761.7 resulting from the monocation $\{[\text{FeL}_3][\text{PF}_6]\}^+$ while the peaks at m/z 548.5 and 521.5 correspond to the species $[\text{FeL}_2]^{2+}$ and LH^+ , respectively. The isotopic patterns of the signals at m/z 809.1 in complex **2** show peaks separated by 0.5 ± 0.1 dalton confirming the existence of a doubly charged species, and the 1.0–1.1 dalton separated isotopic distribution patterns of the peaks at m/z 1761.7 in complex **2** indicate the existence of a singly charged cation. The insets show the comparison of observed (traces) and calculated (bars) isotopic distributions for the major species. In all cases the agreement between experimental and calculated isotopic distribution patterns is excellent and supported the above assignments. The results indicate that the structure of complexes **1** and **2** in solution are the same as those in the solid state which were determined by X-ray diffraction studies.

ES-MS spectroscopy was employed to detect the species produced in the reaction of the ligand **L** with the Ni(II) and Fe(II) ions in solution (at various molar ratios). The ES-MS spectra were recorded for the reaction mixtures of the ligand **L** with $\text{M}(\text{ClO}_4)_2$ at the ratios $\text{M}(\text{II}) : \text{L} = 1 : 4, 1 : 3, 2 : 3, 3 : 3,$ and $3 : 2$, respectively. The ES-MS spectra show that there is no iron(II) or nickel(II) polynuclear complex formed in the reaction mixtures in the presence of an excess of the metal ions, and the species formed in the reaction mixtures are mononuclear complexes. Thus the results show that the linkage of the two 6-substituted 2,2'-bipyridine units at the 5,5'-position of the central bipyridine prevents the formation of polynuclear helical complexes.

Molecular modeling

In order to investigate the possibility of forming a trinuclear complex $[\text{Ni}_3\text{L}_3]^{6+}$ with the ligand **L** molecular dynamic calculations were carried out. The structure of $[\text{Ni}_3\text{L}_3]^{6+}$ (**A**) was built either by shifting the connection of the spacer groups from the β to the α position of the coordinating nitrogens of the terminal bipyridines and all the terminal methyl groups were replaced by hydrogen atoms in structure $[\text{Ni}_3\text{L}'_3]^{6+}$ which was obtained by accessing the X-ray crystal structure data from the Cambridge database or by accessing the crystal structure of complex $[\text{NiL}_3]^{2+}$ and adding two Ni(II) ions which were coordinated by the pendant bipyridine units by the molecular modeling 3D-builder of Cerius². The total energy and the parameters for the resulting minimized structures are almost the same no matter how the original structures were entered. For comparison, the structure of the reported complex $[\text{Ni}_3\text{L}'_3]^{6+}$ (**B**) in which the ligand **L'** contains three bipyridine groups connected by a CH_2CH_2 spacer group at the 5,5'-positions, was built on the basis of the X-ray crystal structure data from the Cambridge database. Since the numbers of the atoms in structure **B** do not equal those in structure **A**, another structure (**C**) which has the same atoms and charge as the structure **A** was built by replacing all the terminal methyl groups with hydrogen atoms in the structure of $[\text{Ni}_3\text{L}'_3]^{6+}$ (**B**), the total energy E and the parameters for the resulting minimized structures **A**, **B**, and **C** were calculated. E_{A} is about 750 kJ mol^{-1} (50%) higher than E_{B} which is about 80 kJ mol^{-1} higher than E_{C} , this implies that it is energetically disadvantageous to form the structure **A** with the ligand **L** compared with the structures **B** and **C**. Furthermore, building a trinuclear triple helix with the ligand **L** resulted in loss of the planarities of all the 6-mono-substituted pyridine groups due to the strain caused by the CH_2CH_2 spacer group, and the largest deviation of the atom from the pyridine plane is 0.2 \AA , whereas the deviation is less than 0.03 \AA for the complex $[\text{Ni}_3\text{L}'_3]^{6+}$ in both the crystal and

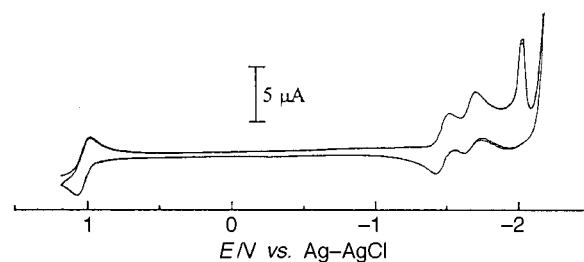


Fig. 3 Cyclic voltammogram of $[\text{FeL}_3][\text{PF}_6]_2 \cdot 2\text{EtOH} \cdot 0.5\text{H}_2\text{O}$ [vs. Ag–AgCl, 100 mV s^{-1} , acetonitrile–0.10 M $(\text{TBA})\text{ClO}_4$].

the modeling structures. In addition the CH_2 carbon atoms of the adjacent terminal bipyridine unit is also out of the parent pyridine plane with distance longer than 0.3 \AA . The results of the modeling and calculations imply that it is geometrically difficult to form a trinuclear complex through linkage of the two 6-mono-substituted bipyridines in the 5,5'-position of the central bipyridine. All the above mentioned results are not unexpected in view of the fact that bipyridines substituted at the 6-position do not easily complex with octahedral coordination centers, but rather with tetrahedral metals like copper(I) and silver(I).

Electrochemical properties of the complexes

Complex **1** shows no voltammetric response in the potential region from 0.0 to 2.0 V in acetonitrile, but exhibits a reversible metal-based redox at $E_{1/2} = -1.30 \text{ V}$ ($\Delta E = 64 \text{ mV}$) vs. Ag–AgCl in CH_3CN solution which is assigned as the $(\text{Ni}^{\text{III}}/\text{Ni}^{\text{II}})$ couple. This is somewhat different from the metal-based redox potential of complex $[\text{Ni}^{\text{II}}(\text{mt-seppy})_2][\text{PF}_6]_4$ ($E_{1/2} = -1.0 \text{ V}$) in acetonitrile [(mt-seppy) = 4',4''-bis(methylthio)-2,2':6',2'' : 6''',2'''' : 6''''',2''''''-sexipyridine].¹⁸ The difference between the $E_{1/2}$ values for these complexes is likely to be due to the different coordination environments. Complex **2** displays four apparent cyclic voltammetric responses as shown in Fig. 3, a reversible metal-based ($\text{Fe}^{\text{III}}/\text{Fe}^{\text{II}}$) redox potential at $E_{1/2} = +1.03 \text{ V}$ ($\Delta E = 56 \text{ mV}$) and three ligand-based redox processes at $-1.45, -1.70,$ and -1.96 V vs. Ag–AgCl in CH_3CN . The $E_{1/2}$ value of metal-based ($\text{Fe}^{\text{III}}/\text{Fe}^{\text{II}}$) redox potential for complex **2** is similar to those of the reported analogs¹⁰ ($E_{1/2}$ values are in the range of 0.923 to 1.062 V) due to the fact that central Fe(II) ions in complex **2** and the reported complexes have a similar N_6 coordination environment and D_3 local symmetry.

¹H NMR Spectra of complex 2

¹H NMR spectra of the ligand **L** and complex **2** in acetonitrile- d_3 at 298 K are shown in Fig. 4. Only one kind of ligand proton signals were observed for **2** within the NMR timescale, although there is a symmetric center for **2** in the solid state. For resolving all the protons of **2**, COSY and NOESY experiments were employed in this work, and peak attributions of the aromatic proton have been assigned as shown in Fig. 4(b). The chemical shifts of the aromatic proton in the complex are different from those in the free ligand. The protons a and b shift downfield by less than 0.16 ppm, while the other protons shift upfield by more than 0.30 ppm, g, j, and h especially shift upfield by 0.63, 0.68 and 2.22 ppm, respectively. Also significant changes occur for the CH_2CH_2 signals, these protons, which appear as a singlet in the free ligand, shift upfield by more than 0.36 ppm and display an ABCD pattern in the complex. Clearly, the protons of each CH_2 group have become non-equivalent in the complex due to the coordination of the central bipyridine group to the Fe(II) ion.

Conclusions

The present study shows that the coordination to metal occurs only at the 5,5'-disubstituted 2,2'-bipyridine moiety of the

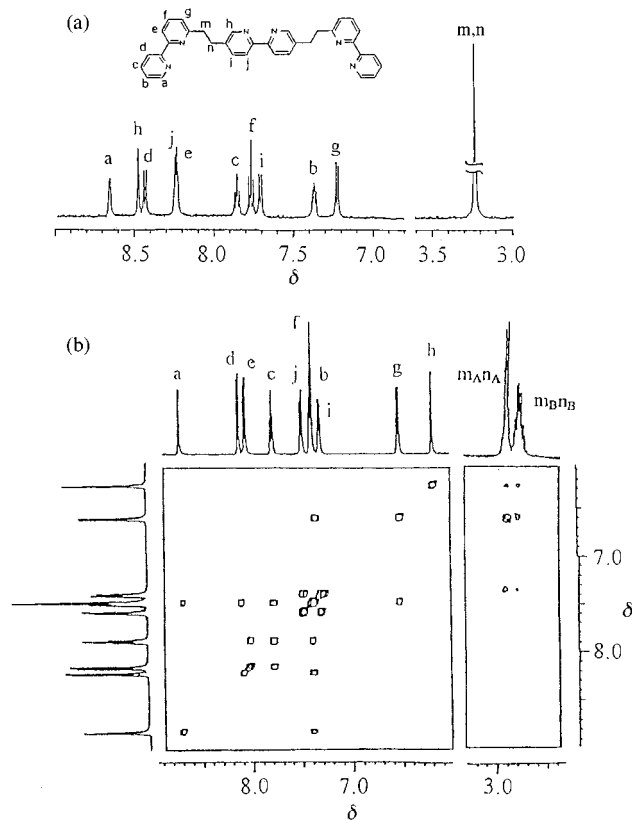


Fig. 4 (a) ^1H NMR spectra of the ligand L in acetonitrile- d_3 at 298 K. (b) COSY (left) and NOESY (right, mixing time: 400 ms) spectra of complex **2** in acetonitrile- d_3 at 298 K.

ligand L and supports the idea that 2,2'-bipyridine units substituted in the 6-position do not easily form complexes with octahedral coordination centers, but rather with tetrahedral metals like copper(I) and silver(I). The results also indicate that the self-assembly process of a helicate not only is related to the coordination geometry of the metal ions and the ligand donor set, but also can be partially controlled by the linkage position of the spacer group to the bipyridine units in oligobipyridine ligands.

Acknowledgements

We are grateful to the National Nature Science Foundation of China for financial support. We thank Prof. Dr. Hoong Kun Fun of X-ray Crystallography Unit, University Sains Malasia for his help in X-ray structural analysis.

References

- (a) F. Vögtle, *Supramolecular Chemistry*, Wiley, Chichester, 1993; (b) J.-M. Lehn, *Supramolecular Chemistry*, VCH, Weinheim, 1995.
- (a) E. C. Constable, *Tetrahedron*, 1992, **48** 10013; (b) C. Piguet, G. Bernardinelli and G. Hopfgartner, *Chem. Rev.*, 1997, **97**, 2005.
- T. Garber, S. V. Wallenda, D. P. Rillema, M. Kirk, W. E. Hatfield, J. H. Welch and P. Singh, *Inorg. Chem.*, 1990, **29**, 2863.
- B. König, M. Zieg, M. Cuntz, L. D. Cola and V. Balzani, *Chem. Ber.*, 1997, **130**, 529.
- M.-T. Youinou, R. Ziessel and J.-M. Lehn, *Inorg. Chem.*, 1991, **30**, 2144.
- (a) J.-M. Lehn, A. Rigault, J. Siegel, J. Harrowfield, B. Chevrier and D. Morras, *Proc. Natl. Acad. Sci. U.S.A.*, 1987, **84**, 2565; (b) U. Koert, M. M. Harding and J.-M. Lehn, *Nature*, 1990, **346**, 339; (c) A. Pfeil and J.-M. Lehn, *J. Chem. Soc., Chem. Commun.*, 1992, 838; (d) C. R. Woods, M. Benaglia, F. Cozzi and J. S. Siegel, *Angew. Chem., Int. Ed. Engl.*, 1996, **35**, 1830; (e) A. Rigault and J.-M. Lehn, *Angew. Chem., Int. Ed. Engl.*, 1988, **27**, 1095.
- T. M. Garrett, U. Koert, J.-M. Lehn, A. Rigault, D. Meyer and J. Fischer, *J. Chem. Soc., Chem. Commun.*, 1990, 557.
- R. Kramer, J.-M. Lehn, A. D. Cian and J. Fischer, *Angew. Chem., Int. Ed. Engl.*, 1993, **32**, 703.
- B. R. Serr, K. A. Anderson, C. M. Elliott and O. P. Anderson, *Inorg. Chem.*, 1988, **27**, 4499.
- S. Ferrere and C. M. Elliott, *Inorg. Chem.*, 1995, **34**, 5818.
- B. Hasenknopf, J.-M. Lehn, N. Boumediene, A. Dupont, G. A. V. Dorsselaer, B. Kneisel and D. Fenske, *J. Am. Chem. Soc.*, 1997, **119**, 10956.
- B. Hasenknopf, J.-M. Lehn, B. O. Kneisel, G. Baum and D. Fenske, *Angew. Chem., Int. Ed. Engl.*, 1996, **35**, 1838.
- J.-C. Rodriguez-U, B. Alpha, D. Plancherel and J.-M. Lehn, *Helv. Chim. Acta.*, 1984, **67**, 2264.
- XSCANS Version 2.1, Siemens Analytical X-ray Instruments Inc., Madison, WI, 1994.
- Siemens SHELXTL Version 5.0, Siemens Industrial Automation, Inc., Analytical Instrumentation, Madison, WI, 1995.
- Cerius², version 3.5, Molecular Simulations Inc., 1997.
- A. K. Rappe, C. J. Casewit, K. S. Colwell, W. A. Goddard III and W. M. Skiff, *J. Am. Chem. Soc.*, 1992, **114**, 10024.
- K. T. Potts, M. Keshavarz, K. F. S. Tham, H. D. Abruna and C. Arana, *Inorg. Chem.*, 1993, **32**, 4436.

Paper 9/01835B